Transactions on Energy Systems and Engineering Applications

Article

Five Level H-Bridge Configuration Based Microgrid with Sugeno Fuzzy Controller for New Energy Generation from Renewable Systems

B. Nagi Reddy[1,*], K. Sarada[2], M. Bharathi[3], Y. Anil Kumar[1], Ch. Rami Reddy[5] and B. Srikanth Goud[4]

1 Department of Electrical and Electronics Engineering, Vignana Bharathi Institue of Technology, Hyderabad, India.
2 Department of Electrical and Electronics, Koneru Lakshmaiah Education Foundation, Vaddeswaram, Guntur, India.
3 Department of Electrical and Electronics, Chalapathi Institute of Engineering and Technology, Guntur, India.
4 Department of Electrical and Electronics Engineering, Anurag University, Hyderabad, India.
5 Department of Electrical and Electronics Engineering, Chonnam National University, Gwangju, South Korea.
* Correspondence: nagireddy208@gmail.com

Received: 28 May 2023; Accepted: 23 June 2023; Published: 10 July 2023

Abstract: Hybrid microgrids run by renewable energy sources are gaining popularity around the world. Solar (PV) and permanent magnet synchronous generator (PMSG) based wind energy systems (WES) are well-known and easy to install renewable energy options. Unfortunately, wind speeds and solar irradiance levels fluctuate unpredictably. Energy generation from both WES and PV panels must therefore fluctuate. Simultaneously, the load is fluctuating irregularly. Hence, storage devices must be incorporated into hybrid systems in order to keep the generation and consumption of electricity in equilibrium. In addition, for a fuel cell and electrolyzer that run on hydrogen, a tiny battery is added into the system to keep costs down. In order to enhance power quality and reliability, all the components in a microgrid need to be connected to an effective energy management system. For optimal use, renewable energy sources are combined with maximum power point trackers. When there are sudden shifts in both the energy supply and demand on a standalone microgrid, the energy balance and frequency response are crucial. In this study, a Takagi Sugeno based innovative fuzzy controller is implemented for a system to manage energy in order to achieve a precious and rapid reaction. The suggested system's Hardware-In-the-Loop is built using OPAL-RT modules in order to demonstrate detailed findings.

© 2023 by the authors. Published by Universidad Tecnológica de Bolívar under the terms of the Creative Commons Attribution 4.0 License. Further distribution of this work must maintain attribution to the author(s) and the published article's title, journal citation, and DOI. https://doi.org/10.32397/tesea.vol4.n2.521

1. Introduction

Everywhere in the world, the need for power is rising rapidly. Similarly, the world is searching for ways to harness non-conventional energy resources to generate electricity in order to meet the demands of users

How to cite this article: B. Nagi Reddy, K. Sarada, M. Bharathi, Y. Anil Kumar, Ch. Rami Reddy and B. Srikanth Goud. Five Level H-Bridge Configuration Based Microgrid with Sugeno Fuzzy Controller for New Energy Generation from Renewable Systems. *Transactions on Energy Systems and Engineering Applications*, 4(2): 521, 2023. DOI:10.32397/tesea.vol4.n2.521

and provide reliable power supplies [1]. In many areas, reducing power demand on utility networks can be accomplished by the installation of renewable energy-based independent microgrids. However, due to the intermittent behavior of renewable sources [2, 3], electrical power generation through a single source cannot supply stable power to the system. Therefore, system reliability can be improved by combining two or more non-conventional energy systems. Solar (PV) and wind energy systems (WES) are the best renewable energy sources and can be found in most parts of the world. Because of its direct coupling to the wind turbine, the PMSG is the best generator for moderate power applications [4]. Due to fluctuations in PV irradiation and wind speed, energy storage devices are essential for ensuring a constant supply.

As a result, batteries are often used with non-conventional energy resources like PV panels and wind turbines. Unfortunately, batteries have a short lifespan (they need to be replaced frequently) and require a lot of upkeep, both of which can increase the long-term cost of operation. The use of an electrolyzer and fuel cell (FC) set for continuous operation in a system with a small enough battery to handle transient power demands is being studied as a solution to these problems. Since the electrolyzer and the fuel cell operate at a relatively sluggish rate, a battery is required to keep the electrical power balance in check and ensure system stability [4]. The system as a whole may be more efficient with such a configuration. However, a robust coordination controller among all the components in a microgrid must be designed to maintain optimal energy balance and power quality.

At some fixed point in time, the gains of the PI controller will be adjusted. For this reason, universal benefits cannot be guaranteed, especially in the case of a microgrid that makes use of variable and intermittent renewable energy sources, an electrolyzer, a fuel cell, a battery, and a load bank. Therefore, Takagi Sugeno based fuzzy controllers are developed, which can have the capability of fine-tuning gains in response to rapid changes happening in the system [5, 6]. Active power can be supplied to loads by any combination of PV, wind, battery, electrolyzer, and batteries [7, 8], but the bulk of loads will require reactive power due to their uses. Therefore, the inverter must correct reactive power via the proposed controller in order to meet load demand. Microgrid frequency is controlled at the point of common coupling (PCC), which also helps achieve active power balance.

The key objectives of this article are:

- A novel coordinated energy management solution was implemented across all microgrid-connected devices.
- Battery, FC, and electrolyzer connections in a microgrid create a cost-effective solution.
- For PV and WES with a limited quantity of sensors, maximum power point tracking (MPPT) systems are implemented.
- TSK-Fuzzy controllers were developed to facilitate quick reactions to unexpected events.
- Two OPAL RT devices were utilized to develop hardware-in-the-loop (HIL).
- The inverter handles both reactive power and frequency compensations.

The research article is structured so that Section 2 reports on the system description as well as an important literature survey. In Section 3, a brief discussion of the design of the TSK-Fuzzy controller, PV and wind MPPT, and inverter controllers of the microgrid is presented. Section 4 presents the HIL-based OPAL-RT results, while Section 5 reports the conclusion.

2. System Description

Systems for generating renewable energy, such as wind and PV power, require MPPT devices with the proper algorithms. As a result, in this study, we explore the step-up topologies for perturb and observe (P&O) algorithms based on MPPT devices for both PV and wind systems. Both the step-up topologies outputs are linked to the DC-link. Charge and discharge currents are controlled by a bidirectional DC-to-DC

topology between the DC link and the battery. Hydrogen is produced according to the quantity of current passing over the electrolyzer. Therefore, a buck converter is connected between the electrolyzer and the DC link in order to boost the current flow. A boost converter is added between the FC and the DC link since the FC operates at a lower voltage. The FC stores the hydrogen and oxygen produced by the electrolyzer in the appropriate tank for use when those elements are required for power production. The AC loads are employed on the DC-link via a three-phase, five-level configuration. To lessen harmonics, an LC filter is attached between the PCC and the inverter. An overview of the microgrid is shown in Figure 1.

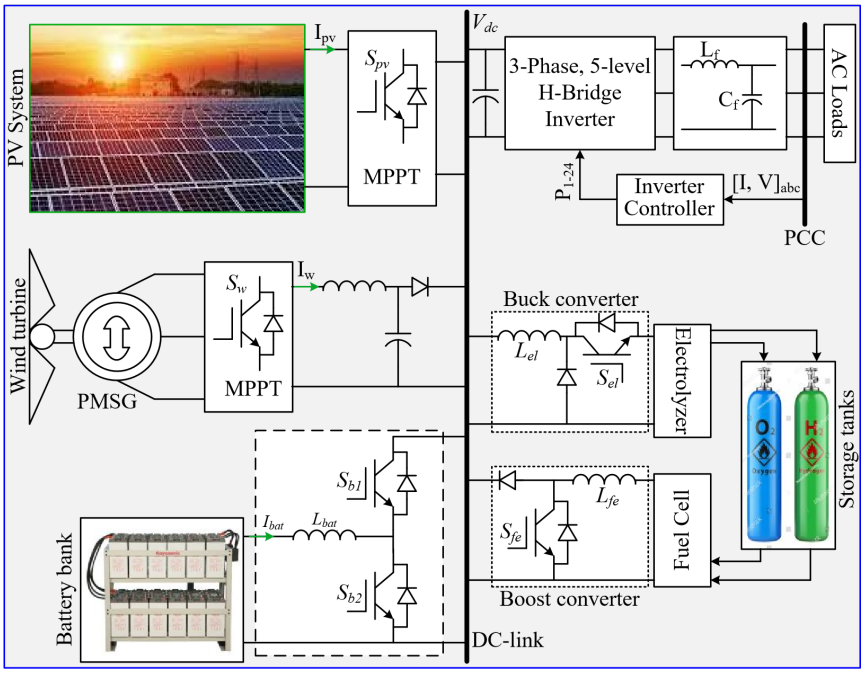

Figure 1. Renewable energy and Battery combined hybrid autonomous microgrid structure.

A few of the authors who have recently published work on similar types of systems are listed here. However, researchers did not take electrolyzer and fuel cell under consideration when implementing new methods for synchronized energy management amongst numerous non-conventional energy sources in the smart grid in Ref [9]. The authors in Ref [10] implemented a synchronization energy supervision system for a PV based hybrid autonomous energy generation system having a fuel cell and an electrolyzer, but the system lacks a WES, and the researchers are more concerned with PV system MPPT than PCC power quality. For an autonomous power generation unit using solar, wind, and batteries, the authors in Ref [11] proposed a 7-level inverter; however, they did not address fuel cells and electrolyzers. Authors in Ref [12] presented the use of batteries in standalone solar-wind hybrid structures, yet the structure is DC microgrid and does not contain an electrolyzer or fuel cell.

The authors in Ref [13] have created a reliable control approach for a hybrid islanding microgrid based on wind and solar energy, but they have left out the electrolyzer, fuel cell, and energy management systems. The authors in Ref [14] discussed a grid-interactive hybrid PV and wind power generation system, although the system is not stand-alone. The authors in Ref [15] created a smart method for energy organization of a PV, battery and wind based DC microgrid; however, the authors do not consider fuel cells or electrolyzers, and the system is not an AC microgrid. In Ref [16], authors offered a system for reactive power flow planning in a hybrid system based on renewable energy sources; nevertheless, the system is deficient in a fuel cell and an electrolyzer. The TSK-fuzzy controller could not be taken into consideration by the authors

in [9]- [16] for quick response, and many of the articles did not use multilevel inverters to improve the voltage profile.

3. Control strategy

3.1. TSK Fuzzy Controller

Due to fixed gains, the PI regulator may not immediately produce an exact reference signal during abrupt changes. Adjusting the weights and gains in response to system changes, TSK-Fuzzy controllers are explicable machine learning tools that are both flexible and powerful. As a result, the TSK-Fuzzy model can reliably produce reference signals despite the presence of stochastic perturbations. ANN learning algorithms are interfaced with the TSK-Fuzzy regulator to obtain frequent weight updates. Figure 2 depicts the implemented block diagram of the TSK-Fuzzy system with an ANN interface, and Figure 3 depicts the weights assigned to each TSK rule. Errors and changes in error rate will be inputs to the system. The proposed TSK-Fuzzy method is defined as

$$f_1 = p_1 X_1 + q_1 X_2 + r_1, \tag{1}$$

$$f_2 = p_2 X_1 + q_2 X_2 + r_2, \tag{2}$$

$$Y = {W_1}^n f_1 + {W_2}^n f_2, \tag{3}$$

where $p_1, p_2; q_1, q_2; r_1, r_2$ are constants which are tuned parameters.

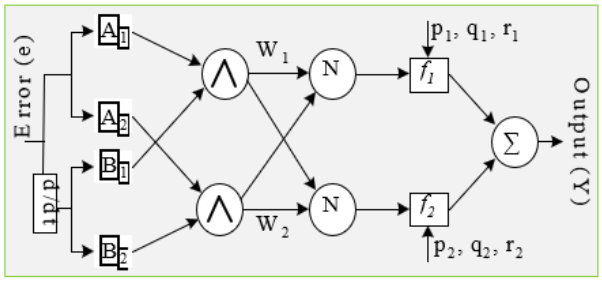

Figure 2. Proposed ANN interfaced TSK-Fuzzy structure.

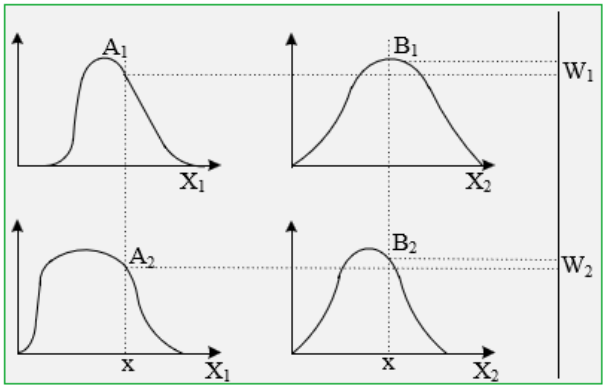

Figure 3. weights of proposed TSK-Fuzzy method.

In order to get a quick reaction, a trained ANN system can adjust the necessary weights. The microgrid's converter controllers can benefit greatly from the TSK-Fuzzy model that has been developed here. TSK-Fuzzy system may take the error signal of the appropriate controller as input and output the useful reference e signal.

3.2. MPPT controllers

Both the wind turbine and PV power vs speed and power vs voltage curves exhibit nonlinearity. Therefore, in order to maximize the potential of both energy sources, it is essential to employ MPPT converters with controllers. The P&O method proves to be a straightforward implementation for a boost converter in a PV system. Consequently, a basic boost converter is integrated into the PV system's connection to the DC-link. The MPPT controller utilizes the DC-link voltage instead of the voltage across the PV structure to minimize the number of required voltage sensors. The simplified architecture of the P&O algorithm for the MPPT controller in the PV arrangement is illustrated in Figure 4. For optimal power output from the wind turbine, it must operate at a specific speed, necessitating regulation by a converter. As the wind turbine's shaft is directly interconnected to the PMSGs, adjusting the PMSG's speed effectively controls the rotational velocity of the wind turbine. Three-phase PMSG generation is converted to direct current (DC) using a controlled rectifier, reducing the number of converters needed. The same rectifier is employed to regulate the current of the PMSG, ensuring it operates at the optimal speed for maximum power output, as the turbine speed depends on the current flow or load. Consequently, the DC current injected into the DC-link from the PMSG serves as a reference for generating 6 pulses (i.e., Sw) using the P&O algorithm, as depicted in Figure 4. The appropriate controller and P&O method for pulse generation to a three-phase controlled rectifier are shown. Since the two MPPT converters may produce different outputs, a diode can be utilized to supply the necessary current to the DC link.

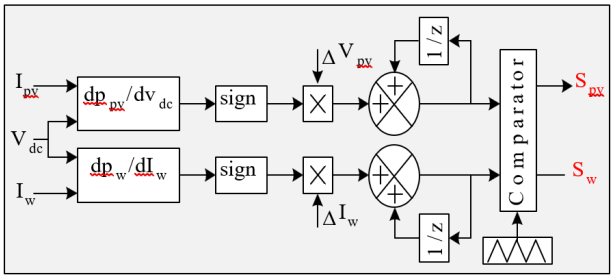

Figure 4. P&O algorithm based MPPT techniques of PV and Wind systems.

The DC-link voltage must be maintained at a constant level. In most cases, DC-link will reflect the energy imbalance between overall generation (including PV & wind power generation) and load. When generation exceeds consumption, the DC-link voltage rises, and when the reverse is true, the DC-link voltage falls. Because of this power disparity between the generator and the load, a battery is linked to the DC-link via a bidirectional DC–DC configuration to control charging and discharging current. Therefore, TSK-Fuzzy controller generates the reference battery current (Ibat*) signal by comparing the DC-link voltage (Vdc) to its reference value (Vdc*). By comparing Ibat* and Ibat, the hysteresis regulator produces the necessary pulses (i.e., Sb1, 2) for the bidirectional DC – DC configuration. In this study, however, we focus on the use of a small battery size to react to transients. Therefore, the battery shouldn't be discharged as well as charged when in steady state operation. Depending on the imbalance between generation and consumption, this may be accomplished with a fuel cell or electrolyzer to store the surplus power. Therefore, pulses for the step-down topology (for electrolyzer) and the step-up topology (for FC) are generated by comparing the Ibat with zero. If the current drawn from the battery is negative, then the production is

greater than the requirement, and if it is positive, then the requirement is greater than the production. By comparing the zero reference signal to the real battery current, the TSK-Fuzzy system generates the duty cycle reference signal for the corresponding converters. In contrast to PI, the proposed Fuzzy controller can immediately account for both negative & positive signs in battery current. Figure 5 shows the corresponding voltage controller for the DC link. When the steady-state current via the battery drops to zero, the FC or electrolyzer can take over. The battery can respond instantly to any change in load, despite the slow dynamics of the electrolyzer and FC.

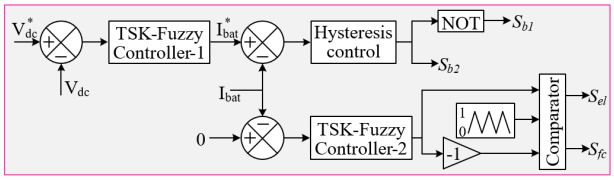

Figure 5. DC-link voltage regulator.

3.3. Inverter controller

Total harmonic distortion can be decreased when an inverter's switching technique is based on Space Vector PWM (SVPWM). In addition, 5-level inverter may be the ideal option for moderate energy applications that need high-quality power and can benefit from the new SVPWM technique [17]. Therefore, this article implements an SVPWM technique based five-level H-Bridge converter to supply AC power to all types of AC loads can be plugged in. Block diagrams of classic 5-level H-Bridge topologies are illustrated in Figure 6.

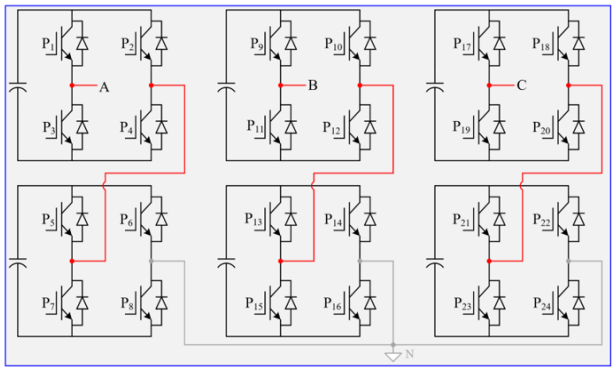

Figure 6. Three-phase, five-level H-bridge configuration.

After the DC-link voltage has been stabilized, the PCC voltage can be maintained by altering the inverter. However, the microgrid's frequency is also crucial; changes in frequency at PCC might be triggered by the active power required by the load. This means that the true part of the load current can be calculated by comparing the reference frequency. Equally, controlling RMS voltage at PCC can compensate for reactive power. In order to create the necessary voltage levels of DQ component via suitable proposed fuzzy controllers, one must first get both real and reactive current component reference signals and then compare these to the real DQ current component. Figure 7 displays the controller diagram in detail for a 5-level inverter. The SVPWM generator will receive the direct and quadrature axis reference voltage signals it needs to generate the correct pulse sequences for the inverter. The pulse sequence of a 5-level configuration is depicted in Figure 8.

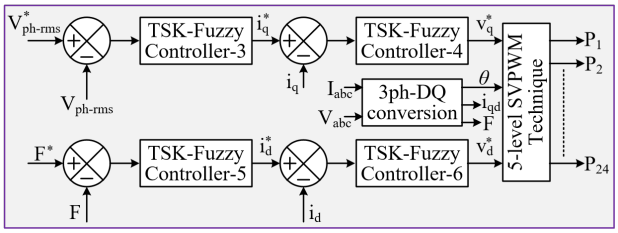

Figure 7. Proposed inverter controller.

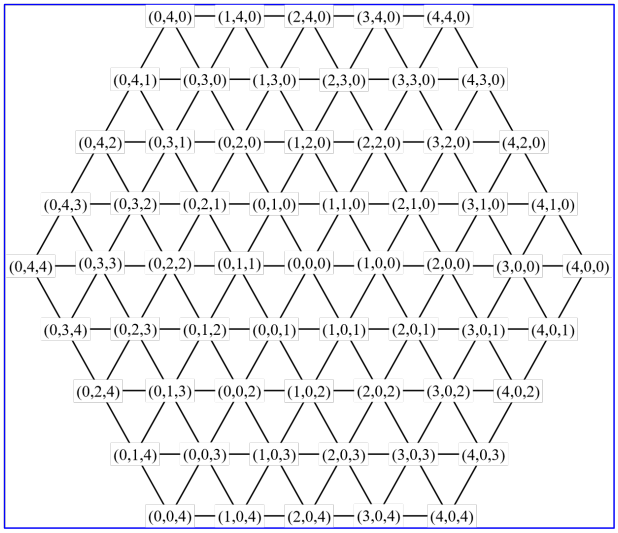

Figure 8. Proposed SVPWM for 5-level configuration.

4. Results and Discussion

In this research, real-time simulators (RTS) are used to enhance the system's performance in a wide range of scenarios. To get an HIL configuration in the lab, researchers use RTS modules like OPAL-RT devices. Two OPAL-RT modules are used to set up HIL for testing proposed complicated controllers in real time. The mass drive train and PMSG parameters are presented in Tables 1 and 2.

The PV array, converters, wind turbine, PMSG, FC, electrolyzer, and AC loads are all dumped into OPAL-RT module 1. Module 2 of OPAL-RT (hence referred to as "OPAL RT-2") contains a dump of all controllers. Through the use of data cards, the plant's analogue signals are transformed to digital and fed into the controller unit (in this case, the OPAL RT-2). The plant's converters can be switched on and off with switching pulses generated by the controller module, which works as intended. Input signals for the plant will be created using analogue conversion of digital pulses from external data cards. To properly present the results, they use a laptop computer instead of an oscilloscope. In Figure 9, we can see the essential HIL configuration, which consists of two OPAL-RT modules. Using the appropriate color coding, Figure 10 describes the laboratory setup for HIL of the proposed system. The designed parameters of the PV and fuel cell systems are presented in Tables 3 and 4. The electrolyzer considered parameters are presented in Table 5.

K_{sh}	0.3 p.u./el.rad
H_t	4s
D_t	0.7 p.u.s/el.rad
H_g	$0.1H_t$

Table 1. Parameters of Two Mass Drive Train.

Rated torque	40 Nm
Number of poles	10
Magnetic flux linkage	0.433 Wb
Rated power	6 kW
Armature resistance (R_s)	0.425Ω
Rated speed	153 rad/s
Stator inductance (L_s)	8.4 mH

Table 2. Parameters of PMSG.

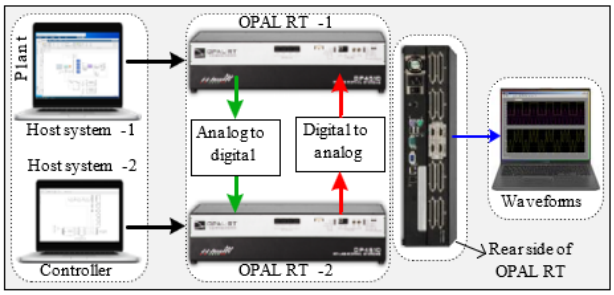

Figure 9. HIL setup with two OPAL-RT modules.

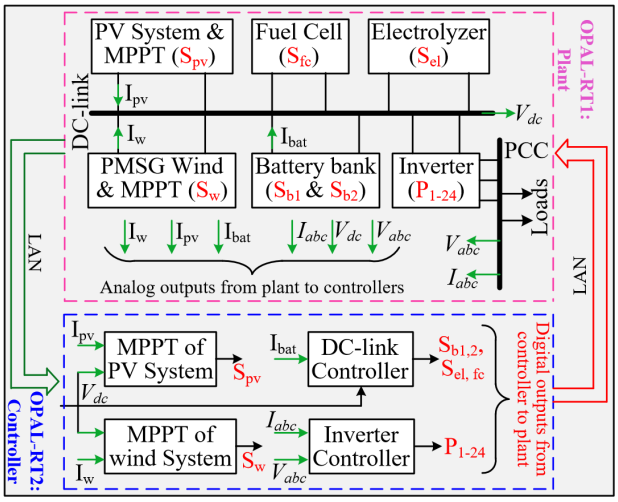

Figure 10. laboratory HIL setup of microgrid with proposed controllers.

Number of modules connected in series/array	15
Short-circuit current (I_{sc})/module	8.01
Current at maximum power (I_{mp_p})/module	7.10
Open circuit voltage (V_{oc})/module	36.90
Voltage at maximum power (V_{mp_p})/module	30.3
Number of arrays connected in parallel/system	2

Table 3. Parameters of PMSG.

Number of cells in series in stack (N_0)	325
Valve molar constant for hydrogen ($[K_H]_2$)	8.43*10-4 (kmol/(s atm)
Ideal standard potential (E_0)	1.18V
Faraday's constant(F)	96487C/kmol
Universal gas constant (R)	8314J/(kmol K)
Valve molar constant for water (K_{H2O})	2.81*10-4 (kmol/(s atm)
Response time for water flow (H_{2O})	78.3 s
Constant, Kr=N0/4F	0.842*10-6 kmol/(s A)
Absolute temperature (T)	1273K
Response time for hydrogen flow (H_2)	26.1 s
Ohmic loss/cell (r)	32813*10-8 Ω
Valve molar constant for oxygen (K_{O2})	2.52*10-3 (kmol/(s atm)
Response time for oxygen flow (O_2)	2.91 s

Table 4. Parameters of Fuel Cell.

N	64
A	873 cm^2
V_{rev}	1.1647 V
r_1	0.00015 Ω m^2
s_1	2.427 V
t_1	0.214 A^{-1} m^2
r_2	-6.019*10^{-6} m^2 $^0C^-1$
s_2	-0.0307 V $^0C^-1$
t_2	-9.870 A^{-1} m^2 ^0C
s_3	3.90*10^{-4} V $^0C^{-2}$
t_3	119.1 A^{-1} m^2 $^0C^{-2}$
T	70 ^0C

Table 5. Parameters of Electrolyzer.

4.1. Case-1: Load variations at PCC

In this example study, we retained the overall generation at 9kW and subjected the system to an AC load variation of 200% at PCC. The following factors, including time and the initial assumption of a 4kW load at PCC, are taken into account when calculating the final load:

First, at time t=3.0 seconds, an 8 kW 3 phase load was unexpectedly attached.

Second, at t=3.16 seconds, we abruptly cut off 8 kW of 3 phase load.

Because of the above-mentioned imbalance between generation and load, the frequency at PCC drops quickly whenever load is attached. The proposed controller quickly and reliably restores the original frequency (in this case, 50 Hz). When the load was suddenly cut off from the PCC, though, the frequency there shot up. Frequency response during the two transitions is shown in Figure 11. As can be seen in this figure, the percentage of variation in frequency is always less than 1%. The frequency of the standalone microgrid is fully stable thanks to the inverter controller that was proposed. Due to the lack of a power grid, the frequency of a freestanding system is typically of paramount importance. By keeping the RMS voltage at the PCC constant, the proposed inverter controller achieves active power balance by keeping the frequency at its reference value. In addition, the inverter controller's TSK-Fuzzy controllers get assistance in achieving a quick response with a small dip/rise in frequency.

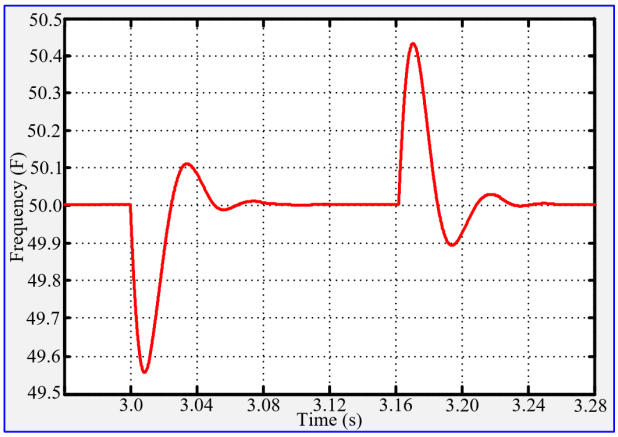

Figure 11. Frequency response with 200% load change.

4.2. Case-2: Irradiance, wind speed and load changes

Variations in solar irradiance, wind speed, and load at PCC are used to calculate the performance of the proposed controllers. This section of the results investigates how the battery, FC, and electrolyzer performed during these variations. At times t=1.5 and 3.0 sec, variations in solar irradiation and wind velocity are taken into account. Power output from PMSG cannot drop precipitously in response to a reduction in wind speed because of the turbine's two-mass design. In Figure 12, we see all the different ways in which the electricity in the standalone microgrid can shift. The events depicted in Figure 12 are as follows:

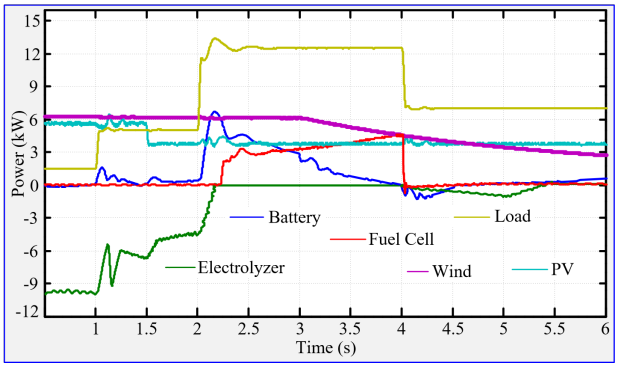

Figure 12. Simulated powers in autonomous microgrid with changes.

The assumed beginning load PCC is 1.5kW at 0.5 sec. It is assumed that PV and wind power are operating at their peak efficiency. Since the generation is larger than the demand, the electrolyzer is using extra electricity. In this case, the negative power indicates that surplus power is being used up. The load has doubled from 1.5 kW to 5 kW in 1.0 seconds.

The battery begins discharging instantly, but the generation is still greater than the load. As a result, electrolyzer power consumption is going down. When the load is suddenly increased, the electrolyzer's power fluctuates for a short period of time due to the battery is discharged even when the load is below the entire power. The solar irradiation drops from 1000 to 700 W/m^2 during time t=1.5 seconds.

Since the electrolyzer is slow to respond, the battery is discharging to try to keep the energy balance. The electrolyzer's electrical usage is lowered until there is an equilibrium between production and load.

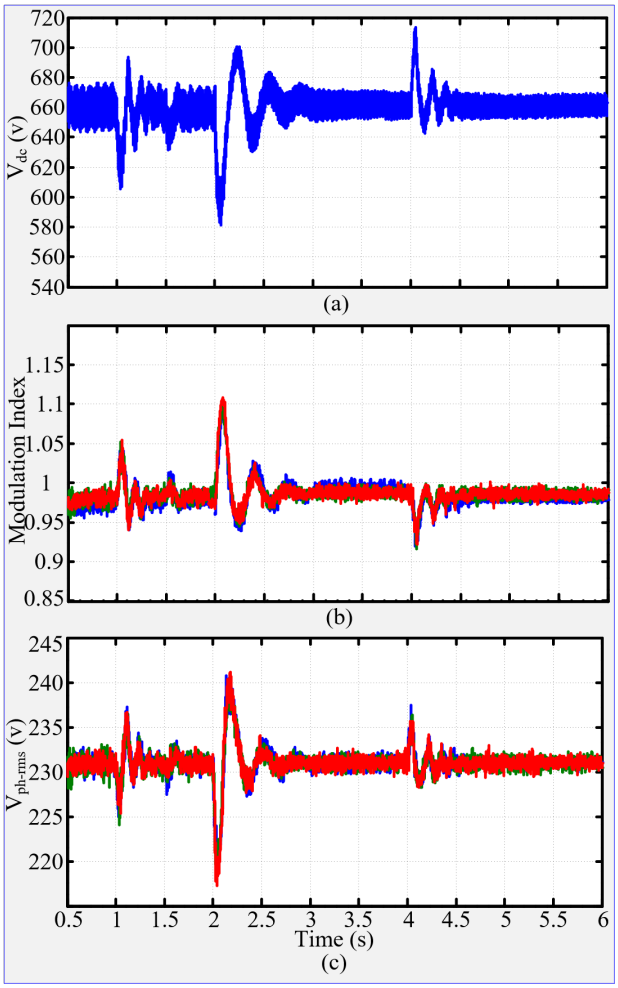

Figure 13. Response of (a) DC-link voltage, (b) modulation indexes, (c) Phase RMS voltages at PCC.

A significant load change occurred at t=2.0 seconds, when the power consumption went from 5kW to 12.5kW. As a result of the adjustment, the battery is reacting rapidly, and power output is falling short of demand. As a result, the battery will try to deplete and the electrolyzer will not use any power at all. However, in order to satisfy load demand, the controller must use FC. Unfortunately, the generation of electricity via FC takes time. So, as shown in Figure 5, the controller gradually raised the electrolyzer's

power output until the battery discharged itself to zero. At t=3.0 seconds, we accounted for the wind's decrease from 12 to 5 m/s.

When wind speeds drop, PMSG's power output falls gradually because of its two-mass drive arrangement, as shown. During this procedure, FC's power generation ramps up to prevent a drop in the power supply.

At time t=4.0 seconds, the load was reduced from 12.5 kW to 7 kW. As soon as there is enough power to go around, the FC stops producing energy, and the battery and electrolyzer take over from there. The DC-link voltage, inverter modulation index, and PCC RMS voltage are all s hown in Figure 13(a), (b), and (c), respectively.

4.3. Case-3: Proposed system response under several changes

Through Fast Fourier Transform (FFT) analysis, we may determine the line voltage and current's total harmonic distortion (THD). From what can be seen in Figure 14, the voltage THD is 3.66 percent. Similarly, Figure 15 depicts the result of obtaining 2.75 percent of the total current. Both of the THD readings are well within acceptable ranges.

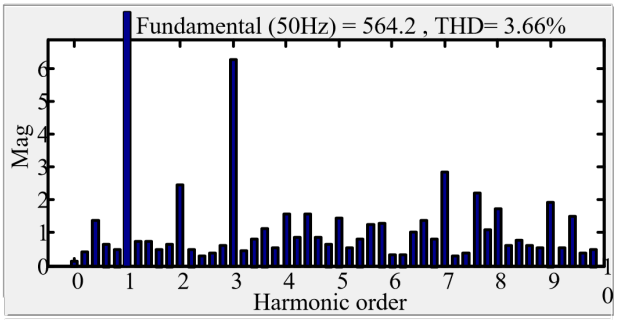

Figure 14. Line voltage %THD.

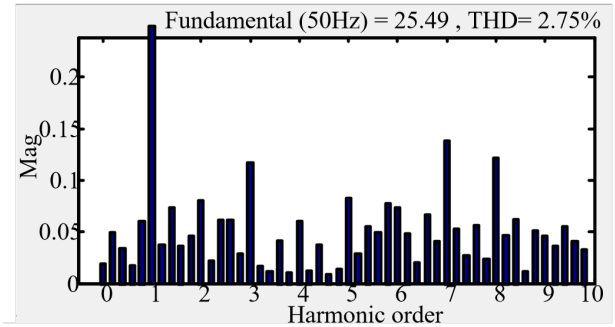

Figure 15. THD of current.

5. Conclusion

For a freestanding microgrid powered by photovoltaics (PV), wind energy, batteries, fuel cells (FCs), and electrolyzers, TSK-Fuzzy controllers are used to construct an efficient energy management system. Proposed controllers are able to obtain a rapid frequency response. All the elements of the microgrid work together as intended thanks to the well-coordinated energy management system. At PCC, the power quality is stable across any transition. A 5-level SVPWM H-Bridge configuration is added to the arrangement to enhance the voltage quality. In the steady-state condition, electrolyzer and FC are supposed to maintain energy equilibrium between production and utility, while a small battery bank is attached to react for

transient phases. Systems using this style of design can improve system dependability and efficiency. In this study, we report HIL results based on OPAL-RT that validate the proposed system in a variety of use cases.

Author contributions: Conceptualization, B. Nagi Reddy and K. Sarada; Software, M. Bharathi; Validation, Y. Anil Kumar, and Ch. Rami Reddy; Formal Analysis, B. Srikanth goud; Investigation, B. Nagi Reddy; Writing – Original Draft Preparation, B. Nagi Reddy; Writing – Review & Editing, M. Bharathi; Visualization, K. Sarada; Supervision, Ch. Rami Reddy.

Disclosure statement: The authors declare no conflict of interest.

References

[1] Ahmad Tazay. Techno-economic feasibility analysis of a hybrid renewable energy supply options for university buildings in saudi arabia. *Open Engineering*, 11(1):39–55, 2020.

[2] Te-Tien Ku, Chia-Hung Lin, Cheng-Ting Hsu, Chao-Shun Chen, Zhan-Yi Liao, Shuo-De Wang, and Fung-Fei Chen. Enhancement of power system operation by renewable ancillary service. *IEEE Transactions on Industry Applications*, 56(6):6150–6157, 2020.

[3] Reddy B Nagi, Sekhar O. Chandra, and Ramamoorty M. Implementation of zero current switch turn-on based buck-boost-buck type rectifier for low power applications. *International Journal of Electronics*, 106(8):1164–1183, 2019.

[4] CN Bhende, Shivakant Mishra, and Siva Ganesh Malla. Permanent magnet synchronous generator-based standalone wind energy supply system. *IEEE transactions on sustainable energy*, 2(4):361–373, 2011.

[5] Jie Li, Longzhi Yang, Yanpeng Qu, and Graham Sexton. An extended takagi–sugeno–kang inference system (tsk+) with fuzzy interpolation and its rule base generation. *Soft Computing*, 22:3155–3170, 2018.

[6] Geuntaek Kang, Wonchang Lee, and Michio Sugeno. Design of tsk fuzzy controller based on tsk fuzzy model using pole placement. *1998 IEEE International Conference on Fuzzy Systems Proceedings. IEEE World Congress on Computational Intelligence (Cat. No. 98CH36228)*, 1:246–251, 1998.

[7] Arobinda Dash, Durgesh Prasad Bagarty, Prakash Kumar Hota, Ranjan Kumar Behera, Utkal Ranjan Muduli, and Khalifa Al Hosani. Dc-offset compensation for three-phase grid-tied spv-dstatcom under partial shading condition with improved pr controller. *IEEE Access*, 9:132215–132224, 2021.

[8] Arobinda Dash, Utkal Ranjan Muduli, Surya Prakash, Khalifa Al Hosani, Sandhya Rani Gongada, and Ranjan Kumar Behera. Modified proportionate affine projection algorithm based adaptive dstatcom control with increased convergence speed. *IEEE Access*, 10:43081–43092, 2022.

[9] B. Srikanth Goud, Ch. Rami Reddy, M. Kondalu, B. Nagi Reddy, G. Srinivasa Rao, and Ch. Naga Sai Kalyan. Islanding detection of integrated dg with phase angle between voltage and current. *Smart Energy and Advancement in Power Technologies*, 926:283–290, 2023.

[10] Chittaranjan Pradhan, Manoj Kumar Senapati, Siva Ganesh Malla, Paresh Kumar Nayak, and Terje Gjengedal. Coordinated power management and control of standalone pv-hybrid system with modified iwo-based mppt. *IEEE Systems Journal*, 15(3):3585–3596, 2020.

[11] Nagaraju Motaparthi and Kiran Kumar Malligunta. Seven level aligned multilevel inverter with new spwm technique for pv, wind, battery-based hybrid standalone system. *International Journal of Emerging Electric Power Systems*, 24(3):389–399, 2022.

[12] Aquib Jahangir and Sukumar Mishra. Autonomous battery storage energy system control of pv-wind based dc microgrid. *2018 2nd International Conference on Power, Energy and Environment: Towards Smart Technology (ICEPE)*, pages 1–6, 2018.

[13] Bhim Singh, Rohini Sharma, and Seema Kewat. Robust control strategies for syrg-pv and wind-based islanded microgrid. *IEEE Transactions on Industrial Electronics*, 68(4):3137–3147, 2020.

[14] Bhaskara Rao Ravada, Narsa Reddy Tummuru, and Bala Naga Lingaiah Ande. Photovoltaic-wind and hybrid energy storage integrated multisource converter configuration-based grid-interactive microgrid. *IEEE Transactions on Industrial Electronics*, 68(5):4004–4013, 2020.

[15] Ahmad Aziz Al Alahmadi, Youcef Belkhier, Nasim Ullah, Habti Abeida, Mohamed S Soliman, Yahya Salameh Hassan Khraisat, and Yasser Mohammed Alharbi. Hybrid wind/pv/battery energy management-based intelligent non-integer control for smart dc-microgrid of smart university. *IEEE Access*, 9:98948–98961, 2021.

[16] Yasaman Niazi, Mohamad Esmail Hamedani Golshan, and Hassan Haes Alhelou. Combined firm and renewable distributed generation and reactive power planning. *IEEE Access*, 9:133735–133745, 2021.

[17] A Suresh Kumar, K Sri Gowri, and M Vijay Kumar. New generalized svpwm algorithm for multilevel inverters. *Journal of Power Electronics*, 18(4):1027–1036, 2018.